



Published in final edited form as:

J Autoimmun. 2018 September ; 93: 45–56. doi:10.1016/j.jaut.2018.06.004.

Protective Role of Commensal Bacteria in Sjögren Syndrome

Mahira Zaheer¹, Changjun Wang^{1,2}, Fang Bian¹, Zhiyuan Yu¹, Humberto Hernandez¹, Rodrigo G. de Souza¹, Ken T. Simmons¹, Deborah Schady³, Alton G. Swennes⁴, Stephen C. Pflugfelder¹, Robert A. Britton⁵, and Cintia S. de Paiva¹

¹Ocular Surface Center, Department of Ophthalmology, Cullen Eye Institute, Baylor College of Medicine, Houston, Texas

²Eye Center, Second Affiliated Hospital of Zhejiang University School of Medicine, Zhejiang Provincial Key Lab of Ophthalmology, Hangzhou, China

³Department of Texas Children's Hospital Pathology, Baylor College of Medicine, Houston, Texas

⁴Center for Comparative Medicine, Baylor College of Medicine, Houston, Texas

⁵Center for Metagenomics and Microbiome Research, Department of Molecular Virology and Microbiology, Baylor College of Medicine, Houston, Texas

Abstract

CD25 knock-out (CD25KO) mice spontaneously develop Sjögren Syndrome (SS)-like inflammation. We investigated the role of commensal bacteria by comparing CD25KO mice housed in conventional or germ-free conditions. Germ-free CD25KO mice have greater corneal barrier dysfunction, lower goblet cell density, increased total lymphocytic infiltration score, increased expression of IFN- γ , IL-12 and higher a frequency of CD4⁺IFN- γ ⁺ cells than conventional mice. CD4⁺ T cells isolated from female germ-free CD25KO mice adoptively transferred to naive immunodeficient RAG1KO recipients caused more severe Sjögren-like disease than CD4⁺ T cells transferred from conventional CD25KO mice. Fecal transplant in germ-free CD25KO mice reversed the spontaneous dry eye phenotype and decreased the generation of pathogenic CD4⁺IFN- γ ⁺ cells. Our studies indicate that lack of commensal bacteria accelerates the onset and severity of dacryoadenitis and generates autoreactive CD4⁺T cells with greater pathogenicity in the CD25KO model, suggesting that the commensal bacteria or their metabolites

Corresponding author: Cintia S. De Paiva, M.D.; Ph.D, Ocular Surface Center, Cullen Eye Institute, Baylor College of Medicine, 6565 Fannin Street, NC505G, Houston, TX 77030, cintiadp@bcm.edu, Phone: 713 798 2124.

Author Contributions: CSDP conceived and designed the experiments; MZ, CW, FB, KTS, HH, RGDS and ZY performed the experiments; CW, FB, DW, MZ, KTS, HH, RGDS and ZY analyzed the data; MZ, DS, KTS, RAB, AGS, SCP, and CSDP wrote the paper.

Presented in part as an abstract at the annual meeting of the 2016 and 2017 Association for Research in Vision and Ophthalmology in Seattle, Washington, and Baltimore, Maryland, respectively.

Conflict of interest

Baylor College of Medicine has filed a provisional patent. No other conflict of interest that could be perceived to bias the work.

The funding sources did not influence the study design; data collection, analysis and interpretation of data; the writing of the report; and in the decision to submit the article for publication.

Publisher's Disclaimer: This is a PDF file of an unedited manuscript that has been accepted for publication. As a service to our customers we are providing this early version of the manuscript. The manuscript will undergo copyediting, typesetting, and review of the resulting proof before it is published in its final citable form. Please note that during the production process errors may be discovered which could affect the content, and all legal disclaimers that apply to the journal pertain.

products have immunoregulatory properties that protect exocrine glands in the CD25KO SS model.

Keywords

Microbiome; Dacryoadenitis; Germ-free; fecal transplant; CD25KO; dry eye; Sjögren Syndrome

1. Introduction

Sjögren syndrome (SS) is an autoimmune disorder that affects exocrine glands, primarily the salivary and lacrimal glands with lymphocytic infiltration leading to dry eye and dry mouth. These glands have significant infiltration that results in apoptosis and loss of secretory acinar cells [1–4]. The infiltrating cells are a mix of T-cells, B-cells, dendritic cells and natural killer cells (NK)[5].

IL-2 receptor alpha chain (CD25) is the binding receptor of IL-2 and the limiting factor of IL-2 signaling [6]. CD25 knock-out (CD25KO) mice display several features of SS, including dacryoadenitis, sialadenitis, and keratoconjunctivitis [7]. These mice develop spontaneous multi-organ inflammatory disease, inclusive of exocrine glands and gastrointestinal tract, and hemolytic anemia that leads to early mortality [8]. CD25KO mice have no IL-2 signaling, lack regulatory T cells and their autoreactive T cells do not undergo activation cell death [7–9]. These mice develop spontaneous dacryoadenitis by eight weeks of age, with 50% lacrimal gland infiltration that progresses to complete atrophy by 16 weeks of age [10]. This age-dependent lacrimal gland destruction is accompanied by increased expression of T cell-related cytokines [10–12]. IFN- γ is critical in this model, as CD25-IFN- γ double-knock-out displayed delayed dacryoadenitis onset and decreased glandular apoptosis while CD25-IL-17 double knock-out had accelerated lacrimal gland destruction [12, 13].

Despite autoimmunity, CD25KO and other mouse models that lack regulatory T cells are susceptible to environmental cues. It has also been shown that in young scurfy mice, a mouse that has a spontaneous mutation in the *Foxp3* gene, oral administration of LPS exacerbated submandibular salivary gland inflammation, providing evidence that microorganisms/microbial products in the mucosa may incite the immune system and trigger autoimmunity. Interestingly, daily oral gavage of scurfy mice with *Lactobacillus reuteri* from day 8 to day 21 significantly improved survival and decreased systemic autoimmunity compared to control mice [7, 14]. A report showed altered eye associated lymphoid tissue in the lacrimal gland of germ-free Swiss-Webster mice, suggesting that microbiota affects mucosal lacrimal gland environment [15]. We have reported that germ-free C57BL/6 mice spontaneously develop Sjögren-like lacrimokeratoconjunctivitis [16].

The microbiome is the ecological community of commensal, symbiotic and pathogenic microorganisms that share our body space. There are trillions of microbes in the body, which account for about 1–3% of total body mass. They play a role in metabolism, homeostasis and maturation of the immune system [17]. In the gut, the microbiome not only helps maintain intestinal homeostasis, it also protects against pathogens and modulates the host's

immune system [18]. Microbial balance and integrity are necessary for good health. The microbiome composition is influenced by environmental factors such as diet, antibiotic therapy and environmental exposure to microorganisms. A loss of balance (dysbiosis) can trigger digestive dysfunctions, allergies and chronic conditions, including obesity and inflammatory diseases [19]. We have previously shown that patients with SS have dysbiosis of their intestinal microbiome, with an inverse correlation between the number of OTUs and the systemic severity score [20].

The purpose of our study was to investigate the role of commensal bacteria in the CD25KO murine model of SS. Herein we describe that the germ-free environment accelerated lacrimal gland lymphocytic infiltration, glandular destruction and accumulation of IFN- γ producing cells. Adoptive transfer of isolated CD4⁺ T cells from germ-free CD25KO mice into RAG1KO mice recapitulated the dry eye phenotype observed in donor mice, demonstrating the protective role of microbiota in spontaneous dacryoadenitis. Furthermore, intestinal microbiota reconstitution of germ-free CD25KO mice decreased generation of pathogenic Th1 cells, suggesting that manipulation of the gut microbiota has the potential to be a novel therapy for Sjögren Syndrome.

2. Material and Methods

2.1 Animals

The research protocol was approved by the Baylor College of Medicine Institutional Animal Care and Use Committee, and it conformed to the standards in the ARVO Statement for the use of animals in Ophthalmic and Vision Research. Germ-free CD25KO (B6;129S4-*IL-2ra*^{tm1Dw}/J) mice were rederived to germ-free status by embryo transfer at Taconic Biosciences and heterozygous F1 mice were delivered to Baylor College of Medicine. Subsequent generations of germ-free CD25KO were produced in the Gnotobiotic Rodent Facility at Baylor College of Medicine. Conventionally housed CD25KO and RAG1KO (Recombination activating gene 1; B6.129S7-*Rag1*^{tm1Mom}/J) breeding pairs were purchased from The Jackson Laboratory (Bar Harbor, ME, USA) for establishing of breeding colonies and raised under specific pathogen free conditions in the standard vivarium. Germ-free mice receive autoclaved LabDiet 5V0F and conventional mice receive irradiated LabDiet 5V5R (PMI Nutrition International, St. Louis, MO). Both groups received water ad libitum, which was sterilized for the animals housed in germ-free conditions.

Conventional and germ-free CD25KO mice of both sexes were used at four (n = 15 and n = 30, respectively) and eight (n = 60; both groups) weeks of age. Six-to-ten week old RAG1KO mice (n = 40) were used as recipients in adoptive transfer experiments. Tissues were collected after euthanasia and used for more than one endpoint whenever possible. Because CD25KO mice have no sex predilection [10], our studies used mice of both sexes.

2.2 Measurement of corneal barrier function

Corneal epithelial permeability to Oregon-green dextran 488 (OGD; 70,000 molecular weight; Invitrogen, Eugene, OR) was assessed as previously described [21]. Briefly, 0.5 μ L of 50 mg/mL OGD was instilled onto the ocular surface 1 minute before euthanasia, then

rinsed with PBS and photographed with a high-resolution digital camera (Coolsnap HQ2, Photometrics, Tucson, AZ) attached to a stereoscopic zoom microscope (SMZ 1500; Nikon, Melville, NY), under fluorescence excitation at 470-nm. The severity of corneal OGD staining was graded in digital images using NIS Elements (version 3.0, Nikon, Melville, NY) within a 2-mm diameter circle placed on the central cornea by two masked observers. The mean fluorescence intensity measured by the software inside this central zone was transferred to a database, and the results were averaged within each group.

2.3 Measurement of Goblet Cell Density

Eyes and ocular adnexa were excised, fixed in 10% formalin, paraffin embedded and were cut into 5- μ m sections using a microtome (Microm HM 340E, ThermoScientific Wilmington, DE USA). Sections cut from paraffin-embedded globes were stained with Periodic Acid Schiff (PAS) reagent. The goblet cell density was measured in the superior and inferior bulbar and tarsal conjunctiva using NIS-Elements software and expressed as the number of positive cells per millimeter per eyelid [22].

2.4 Histology and lacrimal gland inflammation score

Extraorbital lacrimal glands were excised, fixed in 10% formalin, paraffin embedded, and 6- μ m sections were cut as previously described [10]. Sections were stained with Haematoxylin and Eosin (H&E) for evaluating morphology and graded by two masked independent investigators using a modified score described by White and Casarett [23]: 0 = indicated no foci of mononuclear cells was observed; 1 = one to five foci (more than 20 cells per focus); 2 = more than five foci were visible but without tissue damage; 3 = indicated more than five foci with moderate tissue damage; 4 = extensive mononuclear infiltration with severe tissue destruction; 5 = extensive mononuclear infiltration with no normal acini visible.

2.5 Flow cytometry analysis of infiltrating cells

Single-cell suspensions of the lacrimal glands, conjunctival and cervical lymph nodes were prepared as previously reported [16, 24]. CD4, CD8 and B220 cells were stained as previously shown [13, 24, 25].

For intracellular staining, 2×10^6 cells from the single-cell suspensions of lacrimal gland and cervical lymph nodes (n= seven-to-twelve/group) were plated and stimulated by cocktail of Golgi Stop (1ul, Becton, Dickinson and Company, Franklin Lakes, New Jersey, USA), Golgi Plug (1ul, BD), Ionomycin (1ug/ul, Sigma-Aldrich, St. Louis, MO, USA), and PMA (1ug, Sigma-Aldrich, St. Louis, MO), for five hours in a 37°C and 5% CO₂ incubator. After the initial incubation, DNase I (3mg/ml, EMD Millipore Darmstadt, Germany) solution was added for an additional 10 minutes at 37°C. Cells were then moved to 5ml conical tubes and centrifuged for five minutes at 1500rpm. Cells were resuspended in blue live/dead reagent (Invitrogen-Molecular Probes) for 30 minutes in the dark and washed and resuspended in Fixation/Permeabilization (Affymetrix, Santa Clara, USA) solutions up to 18 hours in 4°C. On the next day, cells were permeabilized, stained with anti-CD16/CD32 for 10 minutes on ice, and stained with CD4 (FITC, clone Gk1.5, BD Pharmingen, San Diego, CA), IL-17A (PE, clone eBio17B7, eBioscience, San Diego, CA), IL-13 (eFluor 660, clone:eBio13A, eBioscience), IFN- γ (Pacific Blue, clone XMG1.2, Biolegend, San Diego, CA), and CD45

(Alexa Fluor 700, clone30-F11, Biolegend) antibodies. A BD LSRII Benchtop cytometer was used for data acquisition and data was analyzed using BD Diva Software (BD Pharmingen) and FlowJo software. The following gating strategy was used: live CD45⁺ cells were gated by the exclusion of live/dead dye, followed by two sequential single cell gates. CD4⁺ T cells were plotted again vs. forward scatter area and frequency of Th subtypes were calculated. Biological replicates were averaged.

For IL-12 intracellular staining, single cell suspensions were obtained and 1×10^6 cells were incubated for five hours with one μ L Golgi Stop (BD Bioscience) and one μ L Golgi Plug (BD Bioscience) in 1 mL in complete RPMI, as previously published [16]. Cells were stained with an infra-red fluorescent reactive dye (Life Technologies, Grand Island, NY) for 30 minutes, before fixation. Cells were then stained with CD16/CD32 followed by incubation with anti-CD45 (BV510, clone 30F11, BD Biosciences), anti-CD11c (FITC, clone HL3, BD Biosciences), anti-IL-12 (PE, p40/p70 clone C15.6, BD Biosciences), anti-MHC II (APC, clone IA/IE, BD Biosciences), and anti-CD11b (PE-Cy7, clone M1/70, BD Biosciences). The gating strategy used in this study was as follows: dead cells were excluded by gating live dye versus CD45⁺ cells, subsequently gated by forward scatter height versus forward scatter area (singlets 1), then gated on side scatter height versus side scatter area (singlets 2). IL-12⁺ cells were gated based on forward scatter area and subsequently plotted CD11c and MHC II. The distribution of IL-12⁺ cells was then calculated in the subsets. A BD FACS CANTO II cytometer (Becton Dickinson, San Jose, CA) was used.

Data was acquired with BD Diva software (version 2.1; BD Biosciences) and FlowJo software (version 10.1; Tree Star, Inc., Ashland, OR, USA). Biological replicates were averaged.

2.6 RNA isolation and quantitative PCR

Extraorbital lacrimal glands from germ-free and conventional CD25KO were excised, and total RNA was extracted using a QIAGEN RNeasy Plus Micro RNA isolation kit (Qiagen) following the manufacturer's protocol [10]. The concentration of RNA was measured, and cDNA was synthesized using the Ready-To-Go™ You-Prime First-Strand kit (GE Healthcare). Quantitative real-time PCR was performed with specific minor groove binder (MGB) probes as previously published [21]. Murine MGB probes were IFN- γ (*Iifg*, Mm00801778), IL-1 β (*Iilb*, Mm00434228), IL-12a (*Iil2a*, Mm00434165), major histocompatibility complex class II, MHC-II (*MHC-II*, Mm00482914), TNF- α (*Tnfa*, Mm99999068), IL-23A (*Iil23*, Mm00518984), IL-17A (*Iil7a*, Mm00439619), hypoxanthine phosphoribosyltransferase, HPRT1 (*Hprt1*, Mm00446968). The HPRT-1 gene was used as an endogenous reference for each reaction. The results of real-time PCR were analyzed by the comparative CT method, and the results were normalized by the CT value of HPRT-1.

2.7 CD4⁺ T cell Isolation and Adoptive Transfer

Single-cell suspensions of germ-free and conventional mice were prepared from spleens and draining lymph nodes, and CD4⁺ T cells were isolated by negative selection using rat anti-mouse CD4-conjugated magnetic beads (MACS system; Miltenyi Biotec, Bergisch Gladbach, Germany) following the manufacturer's instructions [26]. Five $\times 10^6$ cells were

injected intraperitoneally into sex-matched RAG-1 KO mice. These mice were euthanized after five weeks, and their tissues were harvested.

2.8 Fecal Microbiota transplant

A fecal microbiota was prepared by collecting fresh stools from C57BL/6J mice into an eppendorf tube containing sterile PBS. Stool pellets were crushed with pipette tips and then centrifuged at 14,000 rpm for five mins. Supernatants were aspirated and fed into mice by oral gavage using intra-gastric needles (100ul/mouse). Oral gavage was performed in 4-week old germ-free CD25KO mice (n = 31) immediately upon exit from the germ-free facility and mice were then housed in the conventional vivarium for another four weeks, when they were euthanized.

2.9 Antibiotic treatment

Four-week old conventional CD25KO or wild-type mice (Jackson Labs, Bar Harbor, ME) were treated with a cocktail of broad-spectrum antibiotics [0.5mg/mL Ampicillin (Dava Pharmaceuticals; Fort Lee, NJ), 0.5mg/mL Gentamicin (Life Tech; Grand Islands, NJ), 0.5mg/mL Metronidazole (Hospira; Lake Forest, IL), 0.5mg/mL Neomycin (Sparhawk Lab; Lenexa, KS), 0.25mg/mL Vancomycin (Hospira; Lake Forest, IL)] dissolved in drinking water with 5mg/ml artificial sweetener (Splenda™, McNeil Nutritionals; Fort Washington, PA) as previously described [27]. Mice received the antibiotic cocktail for 4 weeks and they were euthanized at 8 weeks of age.

2.10 IL-12 neutralization experiment

Germ-free CD25KO mice were randomized to receive bi-weekly i.p. injections of either anti-IL-12p40 antibody (200ug/injection, clone C17.8, n = six) or rat Ig2a isotype control (200ug/injection, clone 2A30, n = six) starting at four weeks of age and biweekly until they were eight week-old, while they were housed in an isolator. Antibodies were purchased from BioXcell, West Lebanon, NH.

2.11 Statistical Analysis

The sample size was calculated using StatMate 2 (GraphPad Software Inc., San Diego, CA, USA) based on pilot studies to have at least 90% power to detect differences with an alpha of 0.05. One-way or two-way analysis of variance (ANOVA), Kruskal-Wallis test with Tukey's post hoc testing, parametric student T or non-parametric Mann-Whitney U tests were used for statistical comparisons with an alpha of 0.05 whenever appropriate using GraphPad Prism 7.0 software (GraphPad Software Inc., San Diego, CA, USA).

3. Results

3.1 Germ-free CD25KO Have Earlier Onset of Lacrimokeratoconjunctivitis than Conventional CD25KO Mice

We have previously shown that CD25KO mice develop lacrimokeratoconjunctivitis, with significant ocular and lacrimal gland alterations [10–12]. Therefore we investigated the role of commensal bacteria by examining ocular and lacrimal gland phenotypes in CD25KO

raised in germ-free conditions and comparing them to CD25KO mice harboring a normal microbiome. We observed that germ-free CD25KO mice have greater corneal barrier disruption and lower conjunctival goblet cell density compared to conventional CD25KO mice at eight weeks of age (Fig. 1A–C). Total lacrimal gland infiltration was measured in histologic sections, and epithelial and acinar death was graded by masked observers, using a modified score described by White and Casarett [23]. Greater lacrimal gland infiltration scores were presented in 4-week old germ-free CD25KO mice, and aging of these mice to 8 weeks further increased their total lacrimal gland infiltration compared to conventional CD25KO mice (Fig. 1D–E). Salivary glands in conventional CD25KO mice had lymphocytic infiltration as previously reported [7, 11]; however, no difference in the submandibular gland infiltration was observed between germ-free and conventional CD25KO mice (data not shown).

The expression of T-cell related and inflammatory cytokines (IL-23, IL-12, IL-17, IFN- γ , MHC-II, TNF- α , and IL-1 β) was evaluated in lacrimal gland lysates by real-time PCR. IL-17A was highly expressed only in the 8-week old conventional mice, while there was no change in the levels of IL-23 (Fig. 1F). IFN- γ and IL-12 increased in conventional and germ-free mice with aging from 4 to 8 weeks; however, this age-related increase was greater in germ-free compared to the conventional group at eight weeks of age (30 vs. 10 fold, respectively). TNF- α and IL-1 β were more elevated in conventional CD25KO mice. Levels of MHC II transcripts were equally elevated in both groups (Fig. 1F).

The cell infiltrate was characterized by flow cytometry in 8-week old conventional and germ-free mice. Flow cytometry analysis demonstrated CD8⁺ T cells were the more abundant cell type, irrespective of age and housing condition (Fig. 1G). There was a significant increase in the frequency of B220⁺ cells in the germ-free CD25KO lacrimal gland compared to conventional CD25KO at 8 weeks of age.

The phenotype of infiltrating CD4⁺T cells was further investigated by intracellular staining and flow cytometry for signature cytokines IFN- γ (Th1), IL-17 (Th17), and IL-13 (Th2) in 8-week old mice. Cells were gated from live, single CD45⁺ cells (Fig. 1H). There was no change in the frequency of CD4⁺ IFN- γ ⁺ cells in lacrimal gland and nodes, although there was a non-significant increase in the cervical lymph nodes of germ-free mice. Th1 cells were the predominant Th subset among Th2 and Th17 cells. A greater frequency of Th1 cells was present in cervical lymph nodes and lacrimal glands of germ-free CD25KO compared to conventional CD25KO mice. We also observed a lower frequency of CD4⁺IL-17⁺ cells in draining cervical lymph nodes (Fig. 1H). These results suggest that commensal bacterial or products produced by them delay the onset of dacryoadenitis in the autoimmune CD25KO mouse strain, while favoring generation of Th1 cells.

3.2 Greater Pathogenicity of Adoptively Transferred Germ-free CD4⁺T Cells in Immunodeficient Mice

Several studies have shown that commensal bacteria play an essential role in the induction of CD4⁺T cell differentiation [17]. We previously demonstrated that adoptively transferred CD4⁺T cells isolated from dry eye mice produced inflammation in the lacrimal glands of naive immunodeficient mice [26, 28, 29]. To investigate if germ-free CD25KO CD4⁺T cells

are more pathogenic than conventional CD25KO cells, CD4⁺T cells were isolated from spleens and cervical lymph nodes and adoptively transferred into sex-matched RAG1KO mice. The dry eye phenotype in the ocular surface and lacrimal gland was investigated five weeks post-transfer in RAG1KO recipients. There was an increased uptake of the fluorescent dye Oregon-green Dextran (OGD) in corneas of germ-free CD4⁺ T cell recipients compared to conventional CD4⁺ recipients, indicating greater corneal barrier disruption in these mice (Fig. 2A–B). This was accompanied by a significant loss of conjunctival goblet cell density in germ-free CD25KO CD4⁺ T cell recipients (Fig 2C). Similar to the phenotype observed in the donor mice, RAG1KO recipients of germ-free CD25KO cells had a higher lacrimal gland total lymphocytic infiltration score compared with conventional CD25KO recipients (Fig. 2D–E). This was accompanied by increased cellular apoptosis and collapse of the acini; some areas of fibrosis were also present (Fig. 2E).

Adoptive transfer recipients of germ-free CD25KO CD4⁺T cells had a higher frequency of CD4⁺IFN- γ ⁺ cells in both cervical lymph nodes and lacrimal glands while a significant decrease in CD4⁺IL-17⁺ cells was noted only in cervical lymph nodes in this group (Fig. 2E). No difference was noted regarding the frequency of CD4⁺IL-13⁺ cells in either site.

Gene expression analysis showed increased expression of IFN- γ , IL-12, MHC II, TNF- α and IL-1 β in the GF CD25KO mice (Fig. 2G), demonstrating greater inflammation and immunogenic changes in the lacrimal gland post-adoptive transfer. There was no change in IL-23 or IL-17A mRNA levels (Fig. 2G) in adoptive transfer recipients.

3.3 Fecal Microbiota Transplant Improves Lacrimal Keratoconjunctivitis and Decreases Pathogenicity of CD4⁺ T cells in Germ-free CD25KO Mice

To determine if commensal microbiota improved disease severity in germ-free CD25KO mice, we performed colonization experiments by transplanting intestinal microbiota as fecal slurry prepared from conventional C57BL/6J mice via oral gavage. Four-week old germ-free CD25KO mice removed from the isolators received the fecal transplant and were subsequently housed a conventional vivarium for another four weeks. Our results showed that germ-free CD25KO mice that received a fecal transplant had significant improvement in corneal barrier function, with OGD staining intensity levels similar to conventional CD25KO mice (Fig. 3A). Similar improvement in goblet cell density and lacrimal gland pathology was seen in germ-free CD25KO mice after fecal transplant (Fig 3B–D).

The amelioration of the dry eye phenotype after fecal transplant suggests modulation of CD4⁺T cell pathogenicity. To test this hypothesis, we performed adoptive transfer experiments where CD4⁺T cells isolated from germ-free CD25KO mice that received a fecal transplant were adoptively transferred to RAG1KO recipients. Similar to our findings in the donor group, adoptive recipients of fecal transplanted CD25KO mouse CD4⁺T cells had lower corneal barrier disruption, lower lacrimal gland infiltration, and a greater goblet cell density than germ-free CD25KO recipients (Fig. 3E–G). Histologic sections of lacrimal glands from recipients of germ-free cells that received the fecal transplant showed a significant improvement in histologic appearance and inflammation score (Fig. 3G–H). In some cases, microbial colonization led to a normal appearing lacrimal gland (Fig. 3H,

mouse#2). This was accompanied by decreased frequency of CD4⁺IFN- γ ⁺ cells in both cervical lymph nodes and lacrimal glands of germ-free CD25KO mice that received a fecal transplant, compared to germ-free CD25KO recipients (Fig. 3I), demonstrating that conventionalization of germ-free CD25KO mice attenuated disease phenotype and generation of pathogenic Th1 cells.

Gene expression in lacrimal glands of recipients of fecal transplanted germ-free CD25KO CD4⁺ T cells also showed a significant decrease in *IFN- γ* , *IL-12*, *MHC II*, *TNF- α* and *IL-1 β* mRNA transcripts (Fig. 3J).

3.4 Antibiotic Treatment of CD25KO Mice Increases the Th1 phenotype in the Lacrimal Gland

Germ-free mice are born and raised in sterile conditions, and lack of bacteria affects immune system development [30, 31]. So far, our results indicate a protective role for commensal microbiota in CD25KO mice, despite lack of regulatory T cells in these mice. To investigate if acute dysbiosis would mimic the results observed in germ-free CD25KO mice, we subjected conventional CD25KO mice to a cocktail of oral antibiotics for four weeks starting at four weeks of age and compared lacrimal gland pathology between conventional CD25KO and antibiotic treated CD25KO mice. Wild-type littermate mice that received the antibiotic cocktail were included as controls. We observed that antibiotic treatment in wild-type mice did not cause lacrimal gland inflammation (Fig. 4A–B). On the other hand, acute ablation of the microbiome by oral antibiotics in CD25KO mice worsened dacryoadenitis compared to untreated CD25KO mice (Fig. 4A–B). Furthermore, gene expression in the lacrimal gland of antibiotic treated CD25KO mice showed a significant increase in *IFN- γ* and *IL-12* mRNA compared to untreated CD25KO indicating that antibiotic-induced dysbiosis in CD25KO mice promoted development of autoreactive IFN- γ -producing immune cells that worsened dacryoadenitis.

3.5 Neutralization of IL-12 in Germ-Free CD25KO Mice Alleviates Autoimmunity

Since we observed modulation of Th1 cells by commensal bacteria, we hypothesized the germ-free environment promoted the generation of Th1 cells through increased production of the Th1 priming cytokine, IL-12. Our results suggests that either lack of education of the immune system by the gut microbiome (germ-free mice, Fig 1G) or acute dysbiosis (antibiotic treatment in conventional CD25KO, Fig 4C) significantly increased IL-12 expression in the lacrimal gland. To investigate the cellular source of IL-12, we performed flow cytometry experiments in cervical lymph nodes, lacrimal glands and conjunctiva, comparing conventional and germ-free CD25KO mice (Fig. 5A). CD45⁺IL-12⁺ cells were gated and subsequently CD11c and MHC II was plotted. We observed an increased frequency of IL-12⁺CD11c⁺MHC⁻ cells in cervical lymph nodes, lacrimal glands and conjunctiva of germ-free CD25KO mice. These results suggest that lack of education of some antigen-presenting cells by microbes modulate IL-12 expression.

Next, we performed antibody neutralization of IL-12 (200ug, twice a week) in germ-free CD25KO mice, starting at four weeks of age for a duration of four weeks. A separate group of germ-free CD25KO mice that were injected with an isotype control antibody in the same

frequency served as a control. We used dacryoadenitis infiltration score as the endpoint since lacrimal gland acini are exquisitely sensitive to IFN- γ induced apoptosis (Figures 1–3 and [13, 32–34]). A decreased lacrimal gland infiltration score was observed in IL-12 depleted germ-free CD25KO compared to isotype injected control mice (Fig. 5C–D). Flow cytometry analysis showed a decreased frequency of Th1 cells in both the cervical lymph nodes and lacrimal glands of anti-IL-12 germ-free treated mice compared to isotype treated control mice. There was no change in the frequency of Th17 and Th2 cells with anti-IL-12 treatment (Fig. 5E). These results indicate that depletion of IL-12, produced by antigen-presenting cells in the germ-free CD25KO model ameliorates the onset and severity of dacryoadenitis by decreasing the generation of CD4⁺ IFN- γ ⁺ cells.

4. Discussion

In this study, CD25KO mice that develop SS-like disease were raised in both germ-free and conventional conditions to investigate the role of the microbiome in ocular and lacrimal gland homeostasis. Germ-free CD25KO mice had greater corneal barrier disruption, lower goblet cell density and earlier onset of dacryoadenitis than conventional CD25KO mice. Furthermore, lack of microbes favored the generation of autoreactive Th1 cells, which produced greater lacrimokeratoconjunctivitis in RAG1KO recipients of germ-free CD25KO T cells. Recolonization of CD25KO with normal stools returned the germ-free CD25KO ocular and lacrimal gland pathology to similar levels observed in conventional CD25KO mice.

Our results showed that germ-free CD25KO have an earlier onset of dacryoadenitis than conventional CD25KO. The effects of the microbiome on the incidence of autoimmune diseases are not well understood and seem to be tissue specific [35–38]. In the female non-obese diabetic (NOD) mouse that develops both type 1 diabetes and salivary gland inflammation, female germ-free non-obese diabetic mice had the same incidence of type 1 diabetes [35, 36], but lower sialoadenitis severity scores than conventional non-obese diabetic mice [37]. Their results and ours suggests that despite being target organs in SS, the immunopathology that develops in these two glands may be differentially modulated by the intestinal microbiota.

Conventional CD25KO had higher expression of IL-1 β and TNF- α (MHC II was not different between GF and conventional mice) at 8 weeks of age compared to germ-free mice. As IL-1 β and TNF- α are also secreted by ductal and epithelial cells, we believe that this increase might be related to dying/apoptotic epithelial cells that are still present in conventional CD25KO mice. The exact point where autoimmunity develops in the donor mouse is difficult to predict; however, the onset of lacrimal gland inflammation is similar in the adoptive transfer experiments when cells are transferred to the recipient at the same time. Therefore, the adoptive transfer experiments allow us to follow the kinetics of disease onset before end-stage disease develops and this may be the reason why adoptive transfer recipients of germ-free cells have higher IL-1 β and TNF- α than conventional CD4⁺T cells recipients.

We further showed a protective role of intestinal bacteria in the lacrimal gland inflammation that develops in the CD25KO. This protective effect was also observed in germ-free C57BL/6J mice, which also develop an SS-like disease that can be modulated by reconstitution of bacteria from wild-type mice [16]. Germ-free IL-2KO mice, a mouse strain with similar phenotypes to the CD25KO strain, displayed increased mortality and significantly increased *IFN- γ* mRNA levels in the colon when they were monocolonized with potentially pathogenic *E. coli*, but not when they were reconstituted with the commensal *Bacteroides vulgatus* [39]. These results indicate how different species and strains of bacteria have differential effects on autoimmunity in the IL-2KO SS model.

Fecal microbiota transplantation from normal C57BL/6J mice to the germ free CD25KO lowered the pathogenicity of their CD4⁺ T cells to the level observed in conventionally housed CD25KO, both in the donor mice, as well as in the adoptive transfer recipients. This indicates that the modulatory effects of the microbiota go beyond the generation of regulatory T cells since CD25KO mice are unable to produce these cells after fecal transplant, as it has been previously shown [40]. One alternative possibility is that bacteria or bacterial products are directly regulating the immune system. In support of our hypothesis, daily oral gavage with the probiotic *Lactobacillus reuteri* DSM17938 from day 8 to day 21 in scurfy mice, a mouse strain with a Foxp3 mutation that is also devoid of regulatory T cells, significantly improved survival compared to untreated scurfy mice (>120 days vs. 25 days, respectively)[14]. This increased survival was accompanied by a decrease in Th1 cells and decreased systemic autoimmunity in liver and lungs.

We identified IL-12, the Th1 inducing cytokine as a factor that may be directly modulated by commensal microbiota. There was a 30 fold increase in IL-12 mRNA levels in 8-week old germ-free lacrimal gland while a 10 fold increase was present in the conventional CD25KO mice compared to 4-week old conventional CD25KO mice (Fig. 1). However, no change was observed in IL-23 neither in the donor nor in the recipient mice, a cytokine that is needed for IL-17 priming and survival [41–43]. Flow cytometry demonstrated that germ-free mice have an increased frequency of IL-2⁺CD11c⁺MHC II⁻ cells in lacrimal glands, draining nodes and conjunctiva compared conventional CD25KO mice. There was no difference in the frequency of Th17 cells infiltrating the lacrimal glands of the donor (Fig. 1H) or recipient mice (Fig. 2F) between germ-free and conventional CD25KO mice, suggesting that the increased pathology in these mice is not due to increased Th17 cells generation. This finding differs from sialadenitis models of Sjögren Syndrome, where a pathological role for IL-17 has been described [44–46]. In the anti-IL-12 experiment that used an anti-IL-12p40 antibody, a decrease in the frequency of Th1 cells was observed in nodes and lacrimal glands, while no change was seen in the frequency of Th17 cells, reinforcing that the improvement in lacrimal gland pathology was due to decreased generation of Th1 cells obtained with the IL-12 depletion. The pathological role of IFN- γ promoting lacrimal and salivary gland acinar health has been described [12, 47–50]. We have previously shown that CD25/IFN- γ double knock-out mice have less severe dacryoadenitis than CD25KO parental strain, a finding previously observed in the NOD mouse model [12, 33].

Taken together, our findings indicate that manipulation of the gut microbiome could be a novel therapeutic option to treat Sjögren syndrome.

Supplementary Material

Refer to Web version on PubMed Central for supplementary material.

Acknowledgments

We would like to thank Leiqi Zhang, Stephanie Fowler, Cynthia Pena-Olivo and Adam Cole for their expert assistance breeding and caring for conventional and germ-free CD25KO mice.

Funding: This work was supported by the NIH/NEY EY026893 (CSDP), Alkek Center for Metagenomics and Microbiome Research (CSDP), Biology of Inflammation Center (SCP and CDP), NIH Training Grant T32-AI053831 (FB), Research to Prevent Blindness Stein Innovation Award (RAB), Research to Prevent Blindness (SCP), Research to Prevent Blindness Departmental Grant (Dept. of Ophthalmology/BCM), The Oshman Foundation (SCP), William Stamps Farish Fund (SCP), The Hamill Foundation (SCP), Sid W. Richardson Foundation, Ft Worth, TX (SCP, CDP), Zhejiang Science and Technology Program of Traditional Chinese Medicine (2015ZB031) (CW), Zhejiang Provincial Medical and Health Science and Technology Program 2015KYA113 (CW) and by the Cytometry and Cell Sorting Core at Baylor College of Medicine, which is funded by the NIH NIAID P30AI036211, NCI P30CA125123, and NCRR S10RR024574.

Reference List

1. Kong L, Robinson CP, Peck AB, Vela-Roch N, Sakata KM, Dang H, et al. Inappropriate apoptosis of salivary and lacrimal gland epithelium of immunodeficient NOD-scid mice. *ClinExpRheumatol*. 1998; 16:675–81.
2. Ishimaru N, Saegusa K, Yanagi K, Haneji N, Saito I, Hayashi Y. Estrogen deficiency accelerates autoimmune exocrinopathy in murine Sjogren's syndrome through fas-mediated apoptosis. *Am J Pathol*. 1999; 155:173–81. [PubMed: 10393849]
3. Kimura-Shimmyo A, Kashiwamura S, Ueda H, Ikeda T, Kanno S, Akira S, et al. Cytokine-induced injury of the lacrimal and salivary glands. *J Immunother*. 2002; 25(Suppl 1):S42–51. [PubMed: 12048350]
4. Zoukhri D. Mechanisms involved in injury and repair of the murine lacrimal gland: role of programmed cell death and mesenchymal stem cells. *OculSurf*. 2010; 8:60–9.
5. Christodoulou MI, Kapsogeorgou EK, Moutsopoulos HM. Characteristics of the minor salivary gland infiltrates in Sjogren's syndrome. *JAutoimmun*. 2010; 34:400–7. [PubMed: 19889514]
6. Taniguchi T, Minami Y. The IL-2/IL-2 receptor system: a current overview. *Cell*. 1993; 73:5–8. [PubMed: 8462103]
7. Sharma R, Zheng L, Guo X, Fu SM, Ju ST, Jarjour WN. Novel animal models for Sjogren's syndrome: expression and transfer of salivary gland dysfunction from regulatory T cell-deficient mice. *J Autoimmun*. 2006; 27:289–96. [PubMed: 17207605]
8. Willerford DMCJ, Ferry JA, Davidson L, Ma A, Alt FW. Interleukin-2 receptor alpha chain regulates the size and content of the peripheral lymphoid compartment. *Immunity*. 1995; 3:521–30. [PubMed: 7584142]
9. Sharma R, Bagavant H, Jarjour WN, Sung SS, Ju ST. The role of Fas in the immune system biology of IL-2R alpha knockout mice: interplay among regulatory T cells, inflammation, hemopoiesis, and apoptosis. *JImmunol*. 2005; 175:1965–73. [PubMed: 16034141]
10. Rahimy E, Pitcher JD III, Pangelinan SB, Chen W, Farley WJ, Niederkorn JY, et al. Spontaneous autoimmune dacryoadenitis in aged CD25KO mice. *Am J Pathol*. 2010; 177:744–53. Epub 2010 Jun 21. [PubMed: 20566743]
11. de Paiva CS, Hwang CS, Pitcher JD III, Pangelinan SB, Rahimy E, Chen W, et al. Age-related T-cell cytokine profile parallels corneal disease severity in Sjogren's syndrome-like keratoconjunctivitis sicca in CD25KO mice. *Rheumatology*. 2010; 49:246–58. [PubMed: 20007286]

12. Pelegriano FS, Volpe EA, Gandhi NB, Li DQ, Pflugfelder SC, de Paiva CS. Deletion of interferon-gamma delays onset and severity of dacryoadenitis in CD25KO mice. *Arthritis Res Ther.* 2012; 14:R234. [PubMed: 23116218]
13. Bian F, Barbosa FL, Corrales RM, Pelegriano FS, Volpe EA, Pflugfelder SC, et al. Altered balance of interleukin-13/interferon-gamma contributes to lacrimal gland destruction and secretory dysfunction in CD25 knockout model of Sjogren's syndrome. *Arthritis Res Ther.* 2015; 17:53. [PubMed: 25889094]
14. He B, Hoang TK, Wang T, Ferris M, Taylor CM, Tian X, et al. Resetting microbiota by *Lactobacillus reuteri* inhibits T reg deficiency-induced autoimmunity via adenosine A2A receptors. *J Exp Med.* 2017; 214:107–23. [PubMed: 27994068]
15. Kugadas A, Gadjeva M. Impact of Microbiome on Ocular Health. *The ocular surface.* 2016
16. Wang C, Zaheer M, Bian F, Quach D, Swennes AG, Britton RA, et al. Sjogren-Like Lacrimal Keratoconjunctivitis in Germ-Free Mice. *Int J Mol Sci.* 2018; 19.
17. Ruff WE, Kriegel MA. Autoimmune host-microbiota interactions at barrier sites and beyond. *Trends Mol Med.* 2015; 21:233–44. [PubMed: 25771098]
18. Hooper LV, Littman DR, Macpherson AJ. Interactions between the microbiota and the immune system. *Science.* 2012; 336:1268–73. [PubMed: 22674334]
19. Burcelin R, Garidou L, Pomie C. Immuno-microbiota cross and talk: the new paradigm of metabolic diseases. *Semin Immunol.* 2012; 24:67–74. [PubMed: 22265028]
20. de Paiva CS, Jones DB, Stern ME, Bian F, Moore QL, Corbiere S, et al. Altered Mucosal Microbiome Diversity and Disease Severity in Sjogren Syndrome. *Sci Rep.* 2016; 6:23561–71. [PubMed: 27087247]
21. de Paiva CS, Chotikavanich S, Pangelinan SB, Pitcher JD III, Fang B, Zheng X, et al. IL-17 disrupts corneal barrier following desiccating stress. *Mucosal Immunol.* 2009; 2:243–53. [PubMed: 19242409]
22. de Paiva CS, Villarreal AL, Corrales RM, Rahman HT, Chang VY, Farley WJ, et al. Dry Eye-Induced Conjunctival Epithelial Squamous Metaplasia Is Modulated by Interferon- γ . *Invest Ophthalmol Vis Sci.* 2007; 48:2553–60. [PubMed: 17525184]
23. White SC, Casarett GW. Induction of experimental autoallergic sialadenitis. *J Immunol.* 1974; 112:178–85. [PubMed: 4544191]
24. McClellan AJ, Volpe EA, Zhang X, Darlington GJ, Li DQ, Pflugfelder SC, et al. Ocular Surface Disease and Dacryoadenitis in Aging C57BL/6 Mice. *Am J Pathol.* 2014; 184:631–43. [PubMed: 24389165]
25. Pitcher J III, de Paiva CS, Pelegriano F, McClellan A, Raince J, Pangelinan S, et al. Pharmacological cholinergic blockade stimulates inflammatory cytokine production and lymphocytic infiltration in the mouse lacrimal gland. *Invest Ophthalmol Vis Sci.* 2011; 52:3221–7.
26. Niederkorn JY, Stern ME, Pflugfelder SC, de Paiva CS, Corrales RM, Gao J, et al. Desiccating Stress Induces T Cell-Mediated Sjogren's Syndrome-Like Lacrimal Keratoconjunctivitis. *J Immunol.* 2006; 176:3950–7. [PubMed: 16547229]
27. Hill DA, Siracusa MC, Abt MC, Kim BS, Kobuley D, Kubo M, et al. Commensal bacteria-derived signals regulate basophil hematopoiesis and allergic inflammation. *Nat Med.* 2012; 18:538–46. [PubMed: 22447074]
28. Zhang X, Chen W, de Paiva CS, Volpe EA, Gandhi NB, Farley WJ, et al. Desiccating Stress Induces CD4(+) T-Cell-Mediated Sjogren's Syndrome-Like Corneal Epithelial Apoptosis via Activation of the Extrinsic Apoptotic Pathway by Interferon-gamma. *Am J Pathol.* 2011; 179:1807–14. [PubMed: 21843497]
29. de Paiva CS, Volpe EA, Gandhi NB, Zhang X, Zheng X, Pitcher JD III, et al. Disruption of TGF-beta Signaling Improves Ocular Surface Epithelial Disease in Experimental Autoimmune Keratoconjunctivitis Sicca. *PLoS One.* 2011; 6:e29017. Epub 2011 Dec 14. [PubMed: 22194977]
30. Smith K, McCoy KD, Macpherson AJ. Use of axenic animals in studying the adaptation of mammals to their commensal intestinal microbiota. *Semin Immunol.* 2007; 19:59–69. [PubMed: 17118672]
31. Al-Asmakh M, Zadjali F. Use of Germ-Free Animal Models in Microbiota-Related Research. *J Microbiol Biotechnol.* 2015; 25:1583–8. [PubMed: 26032361]

32. Tsubota K, Fukagawa K, Fujihara T, Shimmura S, Saito I, Saito K, et al. Regulation of human leukocyte antigen expression in human conjunctival epithelium. *Invest OphthalmolVisSci*. 1999; 40:28–34.
33. Cha S, Brayer J, Gao J, Brown V, Killedar S, Yasunari U, et al. A dual role for interferon-gamma in the pathogenesis of Sjogren's syndrome-like autoimmune exocrinopathy in the nonobese diabetic mouse. *Scand J Immunol*. 2004; 60:552–65. [PubMed: 15584966]
34. Kamachi M, Kawakami A, Yamasaki S, Hida A, Nakashima T, Nakamura H, et al. Regulation of apoptotic cell death by cytokines in a human salivary gland cell line: distinct and synergistic mechanisms in apoptosis induced by tumor necrosis factor alpha and interferon gamma. *JLab ClinMed*. 2002; 139:13–9.
35. Markle JG, Frank DN, Mortin-Toth S, Robertson CE, Feazel LM, Rolle-Kampczyk U, et al. Sex differences in the gut microbiome drive hormone-dependent regulation of autoimmunity. *Science*. 2013; 339:1084–8. [PubMed: 23328391]
36. Wen L, Ley RE, Volchkov PY, Stranges PB, Avanesyan L, Stonebraker AC, et al. Innate immunity and intestinal microbiota in the development of Type 1 diabetes. *Nature*. 2008; 455:1109–13. [PubMed: 18806780]
37. Hansen CH, Yurkovetskiy LA, Chervonsky AV. Cutting Edge: Commensal Microbiota Has Disparate Effects on Manifestations of Polyglandular Autoimmune Inflammation. *J Immunol*. 2016; 197:701–5. [PubMed: 27324130]
38. Consolandi C, Turroni S, Emmi G, Severgnini M, Fiori J, Peano C, et al. Behcet's syndrome patients exhibit specific microbiome signature. *Autoimmunity reviews*. 2015; 14:269–76. [PubMed: 25435420]
39. Waidmann M, Bechtold O, Frick JS, Lehr HA, Schubert S, Dobrindt U, et al. *Bacteroides vulgatus* protects against *Escherichia coli*-induced colitis in gnotobiotic interleukin-2-deficient mice. *Gastroenterology*. 2003; 125:162–77. [PubMed: 12851881]
40. Atarashi K, Tanoue T, Oshima K, Suda W, Nagano Y, Nishikawa H, et al. Treg induction by a rationally selected mixture of Clostridia strains from the human microbiota. *Nature*. 2013; 500:232–6. [PubMed: 23842501]
41. Zheng X, Bian F, Ma P, de Paiva CS, Stern M, Pflugfelder SC, et al. Induction of Th17 differentiation by corneal epithelial-derived cytokines. *J Cell Physiol* 2009. 2009 Sep 10; 222(1): 95–102.
42. Katsifis GE, Reka S, Moutsopoulos NM, Pillemer S, Wahl SM. Systemic and local interleukin-17 and linked cytokines associated with Sjogren's syndrome immunopathogenesis. *AmJ Pathol*. 2009; 175:1167–77. [PubMed: 19700754]
43. Korn T, Bettelli E, Oukka M, Kuchroo VK. IL-17 and Th17 Cells. *AnnuRevImmunol*. 2009; 27:485–517.
44. Nguyen CQ, Hu MH, Li Y, Stewart C, Peck AB. Salivary gland tissue expression of interleukin-23 and interleukin-17 in Sjogren's syndrome: findings in humans and mice. *Arthritis Rheum*. 2008; 58:734–43. [PubMed: 18311793]
45. Nguyen CQ, Yin H, Lee BH, Carcamo WC, Chiorini JA, Peck AB. Pathogenic effect of interleukin-17A in induction of Sjogren's syndrome-like disease using adenovirus-mediated gene transfer. *Arthritis ResTher*. 2010; 12:R220.
46. Lee BH, Carcamo WC, Chiorini JA, Peck AB, Nguyen CQ. Gene therapy using IL-27 ameliorates Sjogren's syndrome-like autoimmune exocrinopathy. *Arthritis ResTher*. 2012; 14:R172.
47. Takahashi M, Ishimaru N, Yanagi K, Haneji N, Saito I, Hayashi Y. High incidence of autoimmune dacryoadenitis in male non-obese diabetic (NOD) mice depending on sex steroid. *Clin Exp Immunol*. 1997; 109:555–61. [PubMed: 9328136]
48. Jabs DA, Lee B, Whittum-Hudson JA, Prendergast RA. Th1 versus Th2 immune responses in autoimmune lacrimal gland disease in MRL/Mp mice. *Invest OphthalmolVisSci*. 2000; 41:826–31.
49. Hayashi T, Shimoyama N, Mizuno T. Destruction of salivary and lacrimal glands by Th1-polarized reaction in a model of secondary Sjogren's syndrome in lupus-prone female NZB x NZWF(1) mice. *Inflammation*. 2012; 35:638–46. [PubMed: 21786007]
50. Meng Z, Klingnam W, Edman MC, Hamm-Alvarez SF. Interferon-gamma treatment in vitro elicits some of the changes in cathepsin S and antigen presentation characteristic of lacrimal glands and

corneas from the NOD mouse model of Sjogren's Syndrome. PLoS One. 2017; 12:e0184781.
[PubMed: 28902875]

Author Manuscript

Author Manuscript

Author Manuscript

Author Manuscript

Highlights

- Germ-free environment worsens severity and accelerates onset of autoimmunity in the CD25KO Sjögren Syndrome Model.
- Germ-free CD25KO mice have greater dry eye phenotype and greater frequency of CD4+IFN-gamma+ cells infiltrating the lacrimal gland than conventional CD25KO mice.
- Adoptive transfer of bulk CD4+T cells isolated from germ-free CD25KO mice cause more severe disease in Rag1KO recipients than conventional CD25KO mice.
- Fecal material transplant in germ-free CD25KO mice decreases dacryoadenitis and ameliorates dry eye phenotype by decreasing generation of pathogenic CD4+IFN-gamma+ cells.
- Neutralization of IL-12 in germ-free CD25KO mice decreases severity of dacryoadenitis.
- Commensal bacteria have a protective role in the CD25KO Sjögren Syndrome Model.

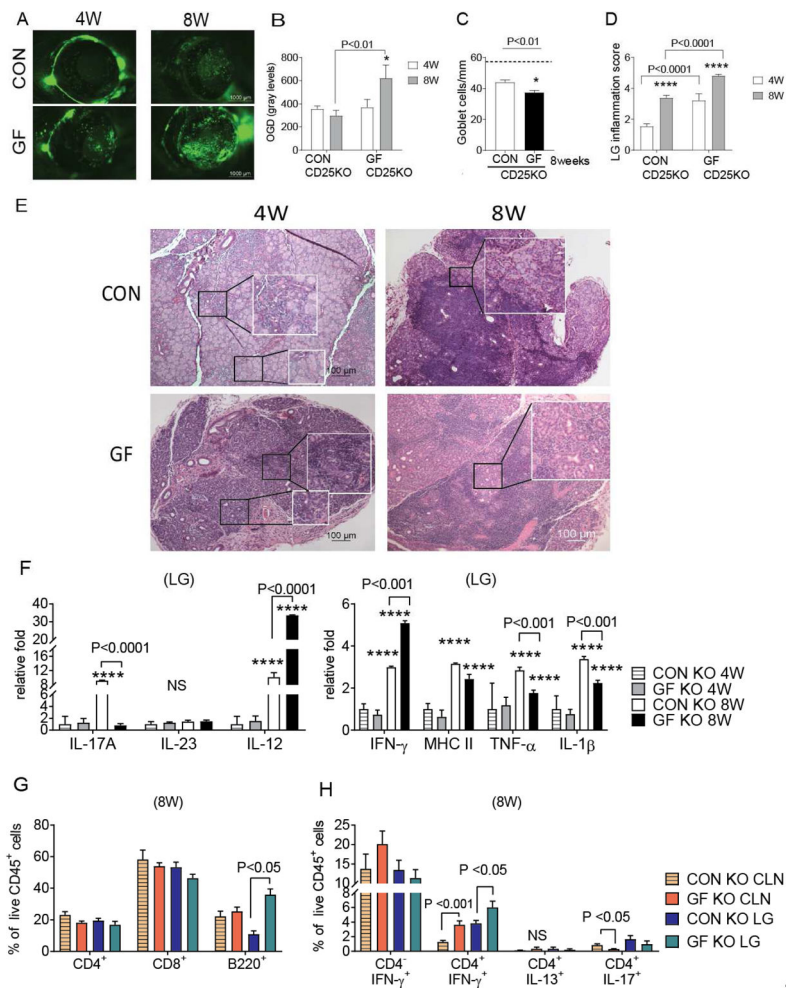


Figure 1. Germ-Free Environment Worsens Sjögren Syndrome in the CD25KO mice

Conventionally (CON) housed CD25KO mice were compared to germ-free (GF) CD25KO mice at four and eight weeks of age. Both sexes were used.

(A–B) Representative pictures of the corneal permeability (A) and accumulative data (B) Corneas were stained with fluorescent Oregon-Green dextran (OGD) dye and OGD intensity score was calculated in the 2-mm central cornea by two masked investigators. Bar graphs show means \pm SEM of two independent experiments with four to ten animals per experiment (final n = nine to twenty animals/group). Parametric t-test were used to make comparisons between groups (p value noted by asterisks). (C) Number of PAS⁺ conjunctival goblet cells counted in paraffin-embedded sections of 8-week old conventional and germ-free CD25KO mice. Bar graphs show means \pm SEM of two independent experiments with three animals per group (final n = six right eyes for each group). Dotted line indicates goblet cell density in wild-type animals. Parametric t- tests were used to make comparisons between groups. (D) Total lacrimal gland score measured in H&E stained sections. Bar graphs show means \pm SEM of three independent experiments with three-six animals per experiment (n = nine to eighteen right lacrimal glands). Nonparametric Mann–Whitney U tests were used to make comparisons of inflammation scores. (E) Representative pictures of haematoxylin and eosin (H&E)-stained sections of lacrimal gland. White quadrants insets are high magnification of

black lined squares. 10X objective. Smaller quadrants are focused on acini appearance. (F) Means \pm SD of gene expression analysis in germ-free and conventional lacrimal gland lysates. Bar graphs show means \pm SD of two independent experiments with a final sample size of five to ten samples per group/age. Two-way Anova with Sidak's post hoc test was used for comparison. (G) Flow cytometric analysis of lacrimal gland stained for CD4, CD8 and B220 at 8 weeks of age. Bar graphs show means \pm SD of two independent experiments, with a final sample size of six samples per group/age. Parametric t-tests were used to make comparisons between groups. (H) Flow cytometric analysis of intracellular staining of lacrimal glands and cervical lymph nodes of conventional and germ-free mice at 8 weeks of age. Right and left extraorbital lacrimal glands from one mouse were excised and pooled into a single tube, yielding a final sample of nine to sixteen individual lacrimal gland samples or nodes divided into four independent experiments with three to-four samples per experiment. Bar graphs show means \pm SEM. Parametric t-tests were used to make comparisons between groups.

*P < 0.05; ***P < 0.001; ****P < 0.0001 age comparison within a group in B, C, D, and F. LG = lacrimal glands; CLN = cervical lymph nodes; NS = non-significant

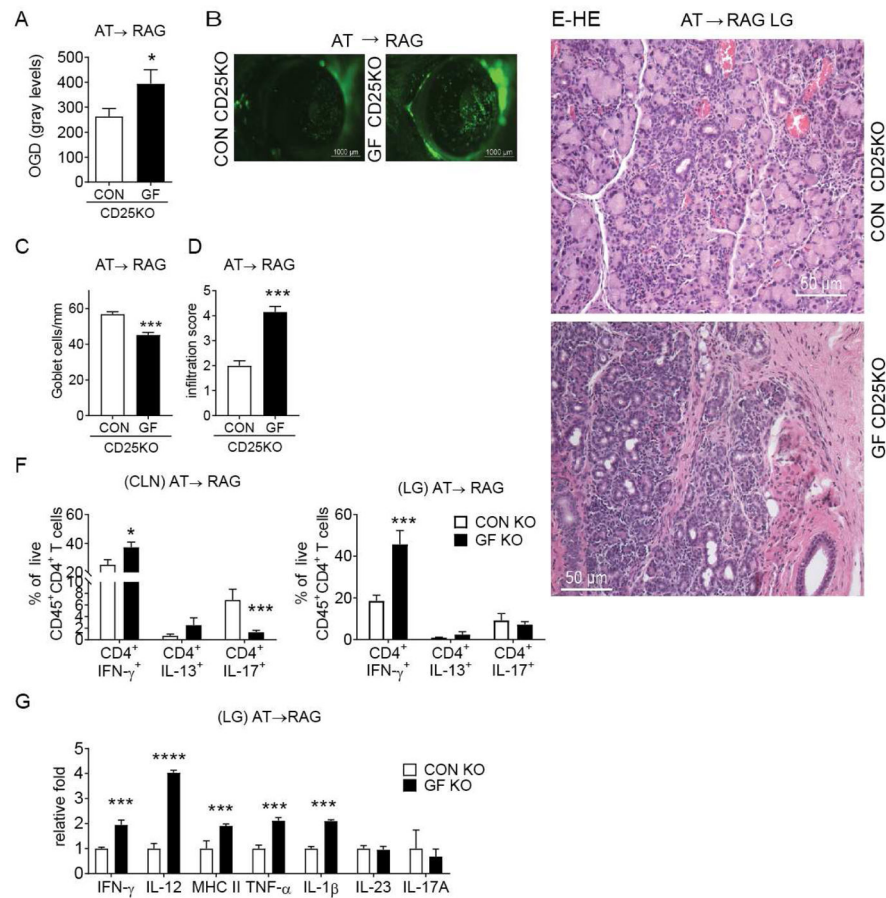


Figure 2. Adoptive Transfer Recipients of Germ-free CD25KO CD4⁺T cells Develop SS-like Disease

CD4⁺ T cells were isolated from spleens and cervical lymph nodes (CLN) from either germfree (GF) CD25KO or conventional (CON) CD25KO mice and adoptively transferred (AT) i.p. into RAG1KO recipients (AT→RAG). Ocular and lacrimal gland phenotype in RAG1KO recipients were investigated 5 weeks post-transfer.

(A) Corneal permeability measured as an uptake of fluorescent Oregon-Green dextran (OGD) dye. Bar graphs show means \pm SEM of two independent experiments with eight to ten animals per experiment (final n = eighteen to twenty animals). Parametric t- tests were used to make comparisons between groups. (B). Representative pictures used to generate the bar graphs in A. (C) Number of PAS⁺ conjunctival goblet cells counted in paraffinembedded sections expressed as number per millimeter. Bar graphs show means \pm SEM of two independent experiments with two to three animals per group, yielding a final sample of five right eyes for each group. Parametric t- tests were used to make comparisons between groups. (D) Inflammation scores of lacrimal gland pathology of donor and AT recipients. Bar graphs show average of two independent experiments (final n = thirteen right lacrimal glands animals). Nonparametric Mann–Whitney U test was used to make comparisons of inflammation scores. (E) Representative pictures of haematoxylin and eosin (H&E)-stained sections of lacrimal gland in adoptive transfer RAG1KO recipients; 20X objective, scale bar = 50 μ m. (F) Flow cytometric analysis of intracellular staining of lacrimal gland and cervical

lymph nodes of adoptive transfer recipients (n= eight to fourteen individual right lacrimal glands). Bar graphs show means \pm SEM of three independent experiments. Parametric t-tests were used to make comparisons between groups. (G) Gene expression analysis in lacrimal gland lysates of germ-free and conventional CD25KO adoptive transfer recipients. (AT \rightarrow RAG). Bar graphs show means \pm SD of two independent experiments (n = eight lacrimal glands/group).

*P < 0.05; ***P<0.001; ****P<0.0001 germ-free vs. conventional comparison

LG = lacrimal gland; CLN = cervical lymph nodes

Author Manuscript

Author Manuscript

Author Manuscript

Author Manuscript

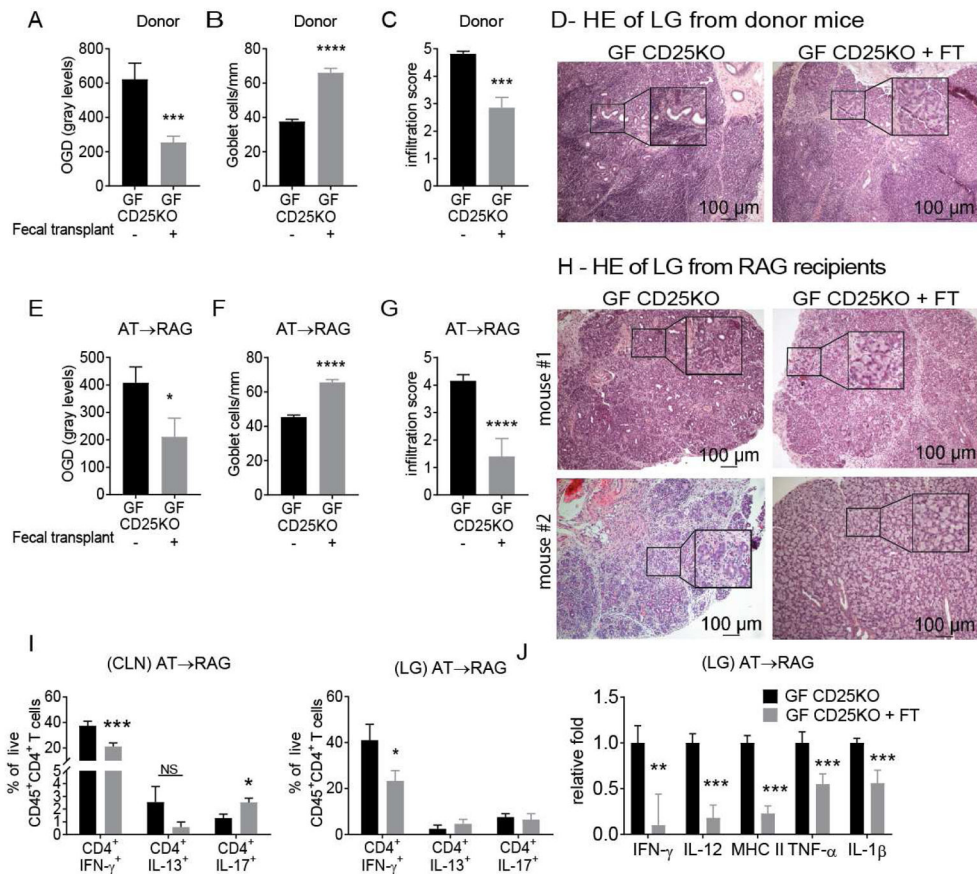


Figure 3. Fecal Microbiota Transplant in Germ-free CD25KO Ameliorates the Autoimmune Phenotype

Germ-free (GF) CD25KO were removed from isolators at four weeks of age and received a fecal transplant (FT) of fecal microbiota and were kept in normal vivarium until they reached 8 weeks of age. CD4⁺ T cells were isolated from spleens and cervical lymph nodes (CLN) and adoptively transferred into RAG1KO recipients (AT→ RAG). Ocular and lacrimal gland phenotype was investigated in both donor mice and RAG1KO recipients. (A–D) Donor mice phenotype after fecal transplant. (A) Corneal permeability measured as an uptake of fluorescent Oregon-Green dextran (OGD) dye. Bar graphs show means ± SEM of three independent experiments (final n = eighteen to twenty-one animals). Parametric t- tests were used to make comparisons between groups. (B) Number of PAS⁺ conjunctival goblet cells counted in paraffin-embedded sections. Bar graphs show means ± SEM of two independent experiments, final n = five right eyes for each group. Parametric t- tests were used to make comparisons between groups. (C) Inflammation scores of lacrimal gland pathology of donor and AT recipients. Bar graphs show average of two independent experiments (final n = ten animals). Nonparametric Mann–Whitney U statistical tests were used to make comparisons of inflammation scores. (D) Representative pictures of haematoxylin and eosin (H&E)-stained sections of lacrimal gland in donor mice. (E–J) Dry eye phenotype in RAG1KO recipients. (E) Corneal permeability measured as an uptake of fluorescent Oregon-Green dextran (OGD) dye. Bar graphs are means ± SEM of two independent experiments (final n = eight to ten animals). Parametric t- tests were used to

make comparisons between groups. (F) Number of PAS⁺ conjunctival goblet cells counted in paraffin-embedded sections expressed as number per millimeter. Bar graphs show means \pm SEM of two independent experiments, final n = five right eyes for each group. Parametric t-tests were used to make comparisons between groups. (G) Inflammation scores of lacrimal gland pathology in AT recipients. Bar graphs show average of two independent experiments (final n = ten animals). Nonparametric Mann–Whitney U statistical tests were used to make comparisons of inflammation scores. (H) Representative pictures of haematoxylin and eosin (H&E)-stained sections of lacrimal gland in adoptive transfer RAG1KO recipients; showing two mice per group. Black quadrants insets are high magnification of smaller black demarcated area. (I) Flow cytometric analysis of cervical lymph nodes and lacrimal gland of adoptive transfer RAG1KO recipients. Bar graphs show means \pm SEM of two independent experiments (final n = seven to eleven animals/group). Parametric t-tests were used to make comparisons between groups.(J) Gene expression analysis in lacrimal gland lysates of adoptive transfer recipients. Bar graphs show means \pm SD of two independent experiments, final n = nine to ten mice/group. Parametric t- tests were used to make comparisons between groups.

*P < 0.05; **P<0.01; ***P<0.001; ****P<0.0001

LG = lacrimal gland; CLN = cervical lymph nodes; NS = non-significant

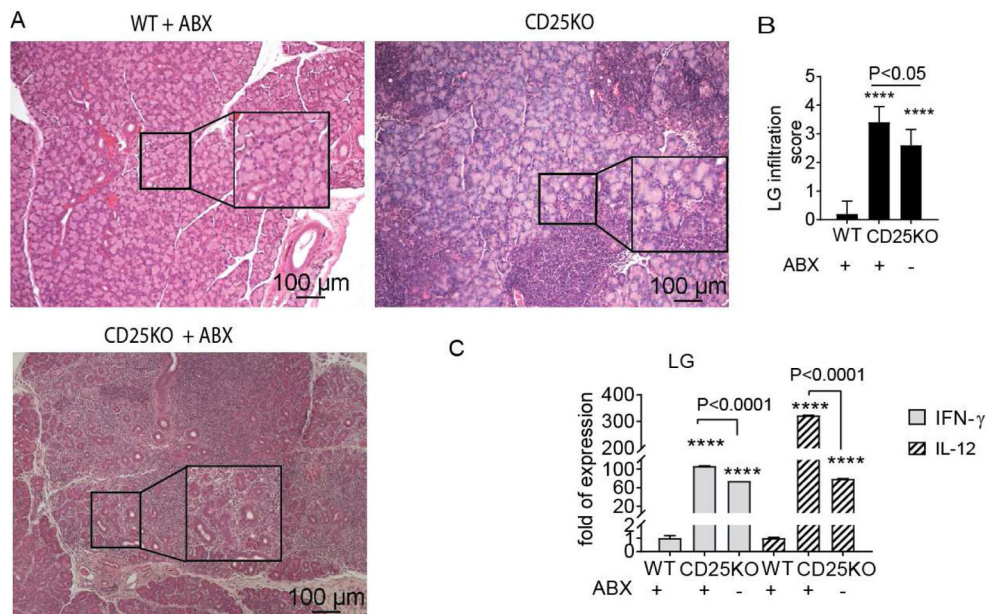


Figure 4. Antibiotic Treatment Worsens Dacryoadenitis in CD25KO mice

Wild-type (WT) and CD25KO mice were subjected to a cocktail of oral antibiotics (ABX) for 4 weeks starting at 4 weeks of age and compared to CD25KO at 8 weeks of age that drank normal water (n = five/group). All groups were born and raised in conventional specific-free pathogen vivarium. (A) Representative pictures of haematoxylin and eosin (H&E)-stained sections of lacrimal glands. Large inset squares are high magnification of small insets, 10X objective, scale bar = 100 μm. (B) Inflammation scores of lacrimal gland pathology. Bar graphs show means ± SEM of two independent experiments, final n = five animals. Nonparametric Mann–Whitney U statistical tests were used to make comparisons. (C) Relative fold of expression of IFN-γ and IL-12 in lacrimal glands. Bar graphs show means ± SEM of five samples per group. Parametric t-tests were used to make comparisons between groups.

****P<0.0001 wild-type vs. CD25KO comparisons (with and without antibiotics)

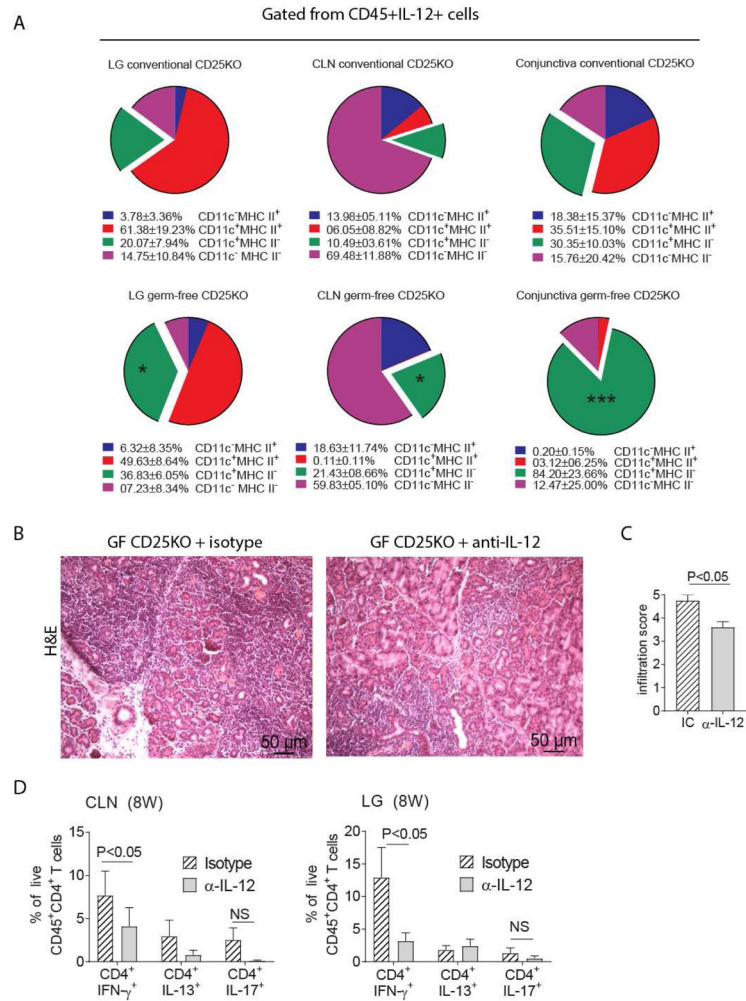


Figure 5. IL-12 Neutralization in Germ-free CD25KO mice Improves Autoimmunity

A-Single cell suspensions were prepared from conventional and germ-free lacrimal glands (LG), cervical lymph nodes (CLN) or conjunctiva and stained with live/dead dye and CD45, IL-12, CD11c, and MHC II antibodies. Single cells, alive CD45⁺IL-12⁺ cells were gated and CD11c and MHC II were plotted.

B–D-Germ-free CD25KO mice, aged four weeks of age, received either anti-IL-12 (α-IL-12) or isotype control (IC) antibody bi-weekly i.p. injections (200ug/injection) for a total of 4 weeks while kept in a germ-free isolator. Mice were used at eight weeks of age (n = six/group).

(A) Flow cytometry analysis showing distribution of CD45⁺IL-12⁺ cells based on CD11c and MHC II expression; pie charts of means of four samples. Means and SD are shown below. Nonparametric Mann–Whitney U tests were used to make comparisons between germ-free and conventional mice, * P<0.05, ***P<0.001.

(B) Representative pictures of haematoxylin and eosin (H&E)-stained sections of the lacrimal gland. 20X objective, scale bar = 50 μm. (C) Inflammation scores of lacrimal gland pathology. Bar graphs show means ± SEM of two independent experiments, final n = five animals. Nonparametric Mann–Whitney U tests were used to make comparisons.

(D) Flow cytometric analysis of cervical lymph nodes and lacrimal gland. Bar graphs are means \pm SD of two independent experiments, with a final sample size of six per group. Parametric t-tests were used to make comparisons between groups.
LG = lacrimal gland; CLN = cervical lymph nodes; NS = non-significant

Author Manuscript

Author Manuscript

Author Manuscript

Author Manuscript